Electrical and Thermal Performance of Different Core Materials Applied in Wind Turbine Blades under Lightning Strikes

Jiangyan Yan[a], Guozheng Wang[b], Yufei Ma[a], Zixin Guo[a], Hanwen Ren[a], Li Zhang[b],

Qingmin Li[a], Joseph D. Yan[c]

[a]State Key Lab of Alternate Electrical Power System with Renewable Energy Sources, North China Electric Power University, Beijing 102206, China;

[b]Weifang Power Supply Company, Shandong Electric Power Corporation of State Grid, Weifang, 261000, China;

[c]Department of Electrical engineering and Electronics, the University of Liverpool, Liverpool, L69 3GJ, UK

Correspondence: Jiangyan Yan, School of Electrical and Electronic Engineering, North China Electric Power University, Beijing 102206, China

Email: yanjiangyan2012@163.com

Conflict of interest statement: Jiangyan Yan and other co-authors have no conflict of interest.

Abstract

Wind turbine blades are subject to lightning strikes, which may result in severe damage of the blade materials. The withstanding performance of different blade materials needs to be classified in order to maximize their operational safety. Lightning impulse voltages were applied to model blades with different core materials (PVC, PET and balsa wood) to characterize the breakdown points (electrically vulnerable areas) on the blades. It has been found that the areas subjected to puncturing are located in the back part (towards the trailing edge) of the sandwich structure, especially at locations close to the main beam. Model blades made of balsa wood are more susceptible to puncturing breakdown than PVC and PET. High impulse currents were imposed at the most probably stricken spots in the impulse voltage tests to compare the severity of damage for PVC, PET and balsa wood, in an attempt to understand the thermal effect of lightning discharge following the final jump. Results show that balsa wood is most resistive to while PVC suffers most damage due to the thermal impact of lightning. Molecular simulation of the chemical degradation process and thermal gas production dynamics was performed at atomic level to explain the damage mechanisms of the three core materials. The performance data of the blade core materials against lightning strike obtained in the present work provide strong guidance on the optimal design of wind turbine blade structure and selection of blade core material.

Keywords: Lightning strike, wind turbine blade, core material, breakdown, material damage, molecular simulation

1 Introduction

With increase in the scale of wind farms, the tip of wind turbine blade can reach a height of 150 metre. When there are no surrounding structures of similar height the wind turbine will be subjected to lightning strikes. According to the faults data collected from wind farms in the USA, each wind turbine suffered 2-3 lightning strikes, on average, on its blades during its whole lifespan[1]. A survey from Oriental Wind Farm in China showed that the lightning fault rate of wind turbines blades reached 5.56% per year[2]. As can be seen in Fig. 1, lightning strikes damaged the blade materials severely, and sometimes resulted in structure cracking. Thus, blade damage is a principal and very severe failure mode among all lightning induced faults as a result of the huge cost involved in the transportation and re-installation of the blades[3]. To certain extent, concerns associated with lightning-induced damages to wind turbine blades have become a major factor hindering further increase in the size and capacity of wind turbines.

There are two types of lightning discharges. The first one is the downward lightning discharge, the leader of which starts from the cloud and moves towards the earth. Most of the natural lightnings are downward lightning. The other is the upward lightning discharge, the leader of which starts from a tall structure on the ground and moves upward to thunderclouds. The latter occurs frequently in areas affected by cold air mass thunderstorms, such as the winter coastal areas in Japan, where the isokeraunic level reaches 30-40[3]. Compared with downward lightning, upward lightning originating from tall structures is likely to have a longer duration of discharge current (more than several tens of milliseconds), and it have caused severe damages on wind turbine blades in Japan[4].

The characteristics of lighting discharge must be fully considered in the design of blade protection, such as the local flash density based on history and the most probable lightning intensity. The most common measure is to use lightning receptors on the blade surface which are connected to earth by a down conductor inside the cavity of the blades. Fig. 2 shows a number of lightning protection concepts[5]. It is hoped that such designs are able to mitigate serious blade damages. When a wind turbine operates in geographic areas with high lightning intensity or high flashover density, especially with the occurrence of positive upward lightning strikes, the receptors and down-conductor needs to be increased in their effective areas to safely discharge the lightning current. It is possible to construct an isolated lightning protection tower on the windward side of a wind turbine when the wind is blown in a relatively constant direction to protect the blades. Research has been performed in Japan [6] and Egypt [7] on lightning protection for wind turbine blades to study lightning attachment on the blade surface. The efficiency of different lightning protection systems were tested with a new countermeasure adopting metallic mesh proposed. Despite of the measures that have been taken there are still a significant number of lightning induced faults reported each year[8]. The situation is worsened when the receptors fail to intercept the last leader of a downward lightning, leading to direct striking on the blade surface with 90% probability on the first 5 metre from the tip[9-12]. It is therefore important to fill the knowledge gap by studying the performance of different blade structures and materials under lighting conditions to improve the lightning defense ability of wind turbine blades.

As for the wind turbine blades, when the lightning leader develops, polarization charge on insulated blade materials and also the induced charge on the metallic receptor or the down conductor exist. The extremely small amount of polarization charge will hardly result in any sensible damage to the blade materials. If the amount of induced charge on the receptor or the down conductor was increased to a

specific level, a leader from the receptor of down conductor may occur and develop towards the direction of the lightning downward leader. The downward and upward leaders develop to each other gradually, and when they are close enough, the air between the will get breakdown, finally, the upward and downward leaders connect to each other. Then large amount of charge is led away through the breakdown channel, and the corresponding thermal and electromagnetic effect will cause severe damage of the blade materials. Modern wind turbine blades have a composite structure featured by laminated sandwich configuration. The laminated components are joined with adhesives. A real blade is shown in Fig. 3a) and a cross-sectional view is provided in Fig. 3b). Normally, a blade consists of two skins, namely the upper and lower blade skin being stuck together, plus two inner webs to hold up the blade structure. The green colored parts in Fig. 3b) represent the main beam and the trailing edge, made of very thick epoxy resin reinforced by glass fiber to guarantee the blade strength. The yellow parts are made of sandwich structures, with core materials in the middle, and two layers of glass fiber are usually wrapped outside. The down conductor is normally laid along the right web towards the ground. According to the data collected from Chinese wind turbine blade manufacturers, currently there are 3 typical core materials used for the blade: polyvinyl chloride (PVC), polyethylene terephthalate (PET) and balsa wood. They are all porous materials and can effectively reduce the weight of wind turbine blade. Among them, PVC is mostly applied because it is the cheapest, while balsa wood is very expensive. Balsa wood is of greater strength than PVC and PET. There are also some blades that use two kinds of core materials, for example, with balsa wood near the blade tip and PVC near the root. However, no standards have been established to regulate the production of blade. PET is relatively new compared with PVC and has not been widely accepted as blade materials due to a lack of important information on its characteristics.

As the downward leader develops from the cloud to the blade (with potential of 0), the electric potential of the cloud will be extended to the leader tip gradually. When the downward leader reaches a specific height, the electric field strength in the space between the downward leader tip and the down conductor in the blade is able to rise to a sufficiently high value to puncture the blade skin when the receptors fail to intercept the downward leader. Once this happens, a huge amount of charge will flow along the breakdown path, leading to energy dissipation in the discharge zone. The peak value of the impulse lighting current and its specific energy can reach approximately 30kA and 55kJ/Ω, which usually lasts for less than 2ms. When the high current goes through the blade skin, it will burn the blade materials severely, resulting in a carbonization area of several millimeters to centimeters in diameter. In particular when a severe impulse voltage punctures into the sealed chamber, the huge thermal effect of the lightning discharge will result in blade edge cracking or rupturing of the whole blade [3, 13-15].

The performance of the different blade materials under lightning strikes, such as breakdown voltage (electrical performance), burned and cracking area (thermal stability), plays a significant role in lightning protection and there is an urgent demand that the prevailing core materials, such as PVC, PET and balsa wood, be extensively tested to affirm their capability against lightning strikes. So far, most of the prevailing research focuses on the attachment characteristics of the receptor and down-conductor system by experiments[16-21], plus large current experiments to study the structural damage of the wind turbine blades[22-25]. However, little research has been done regarding damage mechanism of the blade core materials under lightning strikes, for example, how does breakdown areas distribute, what are the damage characteristics of different core materials and how do the air products and water vapour expansion damage the core materials

In this paper impulse voltage and large current experiments are conducted to study the breakdown

points distribution behavior on different blade samples as well as the damage patterns, characteristics and size. Thereafter, molecular dynamic simulations are carried out to analyze the lightning induced damage mechanisms for different core materials. Combining the experimental and simulation methods, the damage characteristics and mechanisms of different core materials are revealed through comparative study. These findings present technological references in the choice of core materials and structural design of the wind turbine blades against lightning threats.

2 Impulse Voltage Experiments to Explore Breakdown Points

A. Test Samples

To enable meaningful tests conducted in laboratory environment without losing the important features shown in Fig. 3b), the model blades were made into an F-structure with sliced components, each consisting of a plane blade covering and two baffles to hold up the covering, as shown in Fig. 4 and Fig. 5. The covering was made of epoxy resin and porous materials such as PVC, PET and balsa wood by vacuum casting. The overall size of each mode blade is 80cm by 99cm, and the heights were 10cm, 42cm, 35cm and 12cm respectively. Specifically for the sandwich structure, a 0.6cm thick part of PVC, PET or balsa wood was parceled in the middle, plus two layers of 0.9 mm thick glass fiber reinforced epoxy resin being externally wrapped.

B. Test Setup and Procedures

The experimental setup is schematically shown in Fig. 5, where the test sample was placed on a 50 cm high wooden bench. Both the upper and the grounding electrodes were cylindrical with a diameter of 1cm with the latter stuck to the baffle to simulate the down-conductor line inside the blade.

The impulse voltage, in standard parameters of 1.2μs/50μs, were imposed on the test samples with positive and negative polarity. The initial breakdown voltage was first measured. The peak value of the impulse was increased with an appropriate interval until it reached 600kV. The positions of the upper electrode are shown in Fig. 6. Water was sprinkled on the top surface with a moisture level of 0.06g/cm^2 to simulate the thunderstorm weather. In addition, to get more reliable results, each experiment under different peak values of voltage and upper electrode positions was repeated 5 times, and breakdown points were patched using epoxy resin after 5 repeated experiments. With the setup, the weak area that may easily get breakdown under the lightning strikes was comparatively studied and recorded.

C. Results and Discussion

1). Initial breakdown voltage

TABLE I (negative voltage) and TABLE II (positive voltage) give a summary of the initial breakdown voltages in the voltage test experiment. The initial positive breakdown voltages of blade samples with 3 different core materials were obviously lower than the negative breakdown voltages. So positive lightning strikes are able to lead to more serious damage to wind turbine blades. This finding is consistent with the experimental results reported in [6] and [7] which were obtained based on IEC 61400: 2010. The agreement verifies the effectiveness of the present experimental method. It can also be seen that the initial breakdown voltage for balsa wood is slightly lower than that for PVC or PET.

2). Breakdown points distribution

All the breakdown points under negative and positive polarities are shown in Fig. 7 (black stars show breakdown points) and Fig.8. Since the breakdown voltage of a sandwich structure containing PVC, PET or balsa wood was much lower than that of the thick main beam and the trailing edge glass fiber, most breakdown points located in the sandwich area, especially near the intersection arena between the thick glass fiber and the sandwich structure, which is the area near the trailing edge of a real blade. This finding can be verified by CIGRE 578 and real lightning strikes data on wind turbine blades. However, there was only slight difference on the number of breakdown point and their positions between negative and positive voltages.

Repeated experiments show that, the PVC and PET samples are often punctured at the above mentioned locations, while for balsa wood, breakdown tends to take place at different points. This gives rise to a larger number of breakdown points on the balsa wood sample. In addition, multiple branches arcs were discovered in the balsa wood experiments, as shown in Fig. 9. In contrast, this phenomenon seldom happens to the other two samples.

Based on the above experiments regarding the three core blade materials, balsa wood manifests a much larger possibility of being punctured by lightning in the sandwich area. Balsa wood microscopically consists of loose wood fibers, which allows penetrating discharge paths be formed more easily in comparison with foamed PVC and PET. When multiple arc paths occur, the balsa wood blade may be more vulnerable to lightning threats.

3 Large Current Experiments for Material Damage Scenario

As mentioned above, the breakdown points mostly occur in the sandwich area. Hence, sandwich structures with different core materials were studied under large discharge current conditions to gain insight into the severity of damage.

A. Experimental Setup

Both sandwich and combined structures (10cm ×10cm) with different core materials (Fig. 10) were prepared by vacuum casting method, with 0.6cm thick PVC, PET or balsa wood in the middle layer and two layers of glass fiber sandwiching the core material layer.

A hole of 0.18mm diameter was drilled at the middle of the square sample. A nickel chrome wire of 0.01 cm diameter runs through the hole to connect the two electrodes to initiate the high current discharge. The impulse current generator is shown in Fig. 11. Large impulse currents with different source energy (Q) of 199.5J, 1795.5J and 3192J, which had enough energy to damage the blade materials like natural lightning strikes, were applied to simulate the strong thermal impact of the lightning discharge inside the blade materials, with a view to revealing the damage mechanism.

B. Results and Discussion

1). Damage morphology of the sandwich structure

After experiencing large impulse current, all the tested samples exhibited damage of different extent. The PVC and PET sandwich samples show much more severe damage compared with the balsa wood

samples, as can be seen in Fig. 12, The PVC appeared to have suffered the worst case. When the current source energy increased to 1795.5J and 3192J, the PVC and PET material nearby the nickel chrome wire became chemically carbonized, and the whole sample sliced into two parts due to the impact of strong thermal flow and the explosive nature of the discharge.

A unique feature was found for the case of balsa wood samples. When the impulse current source energy were 199.5J and 1795.5J, only a tiny part started to layer nearby the nickel chrome wire. With the highest energy of 3192J, only one edge cracked in the interaction area between the glass fiber and the balsa wood and there was almost no black carbonization phenomenon there, refer to Fig. 12i).

To give a quantitative comparison of the three materials in terms of the endurance capability under large impulse currents, a tolerance index was defined as the area ratio between the non-layering part and the whole sample, as is shown in TABLE III. It can be seen that, balsa wood has much bigger tolerance ratio than the other two materials when the current energy was increased from 199.5J to 1795.5J or 3192J.

2). Damage morphology of the combined structure

As can be seen from Fig. 13, 14 and 15, for the combined samples, most damaged parts are located at places where porous materials are present in the sandwich structure. When the impulse current energy increased to 3192J, the glass fiber began to layer apart. However, the layering area of the three samples showed different ratio values, as can be seen in TABLE IV. The balsa wood sample still performed the best among all the three samples, while the PVC combination sample showed the lowest tolerance radio by experiments.

3). Discussion

According to the above experiments, the balsa wood samples present preferable advantages to the PET and PVC samples in withstanding the thermal blast damage of the impulse current. The PVC samples performed the worst out of the three. Therefore, the wind turbine blade adopting PVC and PET in sandwich structure would suffer much more severe layering and burning under the same lightning strikes. Normally the glass fiber itself is strong enough to resist the thermal blast, however, it may also suffer from layering apart because of the violent gas expansion incurred from the thermal explosion in the porous materials, especially for PVC and PET. To account for the damage mechanism of the three samples from a microscopic viewpoint, a molecular simulation methodology was utilized for a further study.

4 Molecular Simulation on the Damage Mechanism of Different Blade Materials

In addition to the high density thermal energy and the associated thermal blast, chemical reactions including pyrolysis occurs, which leads to materials degradation and mechanical damage.

A. Simulation Setup

To facilitate a comparative simulation, the corresponding parameters of PVC, PET and balsa wood are listed in TABLE V.

A simulation system was established and an identical volume was assumed of the three materials. Also, to reduce computing time while without losing generosity, 10 PVC molecules, 3 PET molecules

and 2 cellulose molecules were, respectively, added into the simulation model. 4 repeated units were set as per type of molecules, denoting that the degree of polymerization (DP) is 4. The number of the water molecules for the three cases was set, respectively, to 2, 2 and 8 based on the materials' actual moisture. The simulation model was implemented on the ADF software specialized for RMD simulation, as shown in Fig. 16. Since the arc temperature might reach several thousands degree, the pyrolysis process at 4998K, 2898K and 498K (around the glass transition temperature of three materials) was simulated for a duration of 100ps using ReaxFF in the ADF platform. ReaxFF denotes the reaction force field in the ADF software, in which bonds breaking and recombination between the atoms can be predicted by calculating the correlations between bond length, bond order and bond energy. Hence, it is an effective method to simulate the chemical reaction process of materials degradation. All the atoms are shown in a stylish way of balls and sticks, where C atom is grey, H atom is white, O atom is red and Cl atom is green.

B. Simulation Results

1). Pyrolysis denoted by degree of polymerization (DP)

It can be seen from Fig. 17 that the PET molecular chains begin to break into several radicals at 498K, and several H and Cl atoms defach from the PVC chain, delivering HCl molecules. The cellulose only exhibits breaking off due to its preferable thermal stability. When the temperature increases to 2898K and 4998K, the PVC and PET are carbonized into carbon skeleton and thereby turn black. This corresponds to the case seen in Fig. 12 in the large current experiment. On the other hand, balsa wood does not suffer severe carbonization, and that is why blackened areas of balsa wood was much smaller than that of PVC and PET in experiment. Although several PVC molecules break into smaller ones, some remnant C-chains are still connected to each other and increases the DP instead. DP is a very useful parameter to reflect mechanical strength of the polymers. In the pyrolysis process, the average DP was recorded, and thereafter the residual DP ratio between the average DP and the initial DP was calculated, as shown in Fig. 18. For PVC samples, there is no sensible reduction of the mechanical strength due to its own chemical degradation. However, the DP of PET and Balsa wood decreases sharply according to the simulation results, especially the PET sample showes an even larger decreasing rate of DP.

2). Gas products

Previous work[26] indicated that, hydrocarbon with more than 5 C-atoms or CHO compounds with more than 1 C-atom, usually form fluid tar in the cellulose pyrolysis process, hence, the products with less C atoms than the above compounds, H_2O and HCl are defined as gas products in this paper. All generated water and added water is considered as vaporous water. The obtained gas products by simulation are shown in Fig. 19. It can be seen that, only PVC and PET chemically generate some gas products at 498K, while all the gas products of cellulose come from the vaporous water at 498K. When the temperature increased to 2898K and 4998K, the cellulose would generate as many gas molecules as PVC, and in these cases PET tendes to produce the least amount of gas products among the three materials.

C. Discussion

Combining the simulation and experiments results, the damage mechanism of the three core materials can be revealed comparatively as following: firstly, the PET and balsa wood samples experienced more severe chemical pyrolysis that reduces their mechanical strength, while the residual

DP of PVC does not change so much under the same simulation temperature; gas blast under impulse current discharge is another important factor to cause the blade material damage. If the temperature is below 498K, balsa wood hardly generates any gas products, while the PET and PVC samples will produce some small gas molecules. When the temperature reaches 2898K and 4998K, the gas products impose more serious threat for balsa wood than for PET or PVC. However, balsa wood still performs the best under large current discharge experiment among the three, due to its sparse wood fiber structure, in which the explosive air flow can be well pinched away, hence, the samples usually get laminated at the interface between the balsa wood and the glass fiber reinforced resin, but not so much inside the balsa wood itself. This may serve as an explanation why the balsa wood gets the least damage among the three in the experiment even if it may degrade severely and generate more gas products. The PVC and PET samples are both in foam structures with closed pores, so they suffer much more severe cracks resulting from gas expansion. Especially for the PVC sample, since it has larger porosity and produces more gas products, the sample suffers more severe gas expansion damage than PET.

5 Conclusions

The present work aims for a comparative study on the performance against lightning strikes of three prevailing core materials used in wind turbine blades. The breakdown point distribution and damage scenario were obtained by experiments and the damage mechanism is explored using RMD simulation.

(1) The sandwich structure on the wind turbine blades especially the one near the trailing edge is an electrically weak area suffering from breakdown discharges under imposed impulse voltage. The receptors installed near the front edge of the blade need to be optimized for an improved efficiency.

(2) Balsa wood is the weakest of the three materials to withstand the lightning voltages and multiple arc discharge paths may occur. However, balsa wood shows preferable thermal stability to PVC and PET in large impulse current discharges. PVC has similar electrical strength to PET, but it behaves worse and gets more severe damage than PET due to the thermal impact. Therefore PVC is not suggested to be used widely in terms of lightning protection. In addition, cost is another important factor that should be considered. The findings present referential basis for material selection and mechanical structure design in terms of lightning withstanding capability and protection measures.

(3) The damage mechanism of the three core materials manifest different causes. For PVC, chemical pyrolysis does not reduce its mechanical strength very much at the temperature used in simulation, and the severe damage is mainly attributed to the gas expansion inside the closed pores. For PET, it may degrade severely under the thermal blast impact of the impulse currents, and its closed pores will further aggravate the severity of the damage. For balsa wood at high temperatures, it will generate large amounts of gas products and its degree of polymerization (DP) decreases sharply. However, balsa wood may suffer less damage compared with the other two, because the relatively loose fiber structure allows gas to escape easily. In general, the physical and chemical structure of the core materials plays a dominant role in determining the degree of damage, and thereby specially designed porous structures may preferably be chosen for the turbine blades so as to guarantee sufficient tolerance against lightning threats.

6 Acknowledgement

The authors would hereby express their appreciations for the financial support by the National Natural Science Foundation of China (51420105011) and (51677110).

7 References

[1] A. C. Garolera, S. F. Madsen, M. Nissim. Lightning Damage to Wind Turbine Blades From Wind Farms in the U.S.. *IEEE Transaction on Power Delivery.* 2016; 31(3): 1043-1049.

[2] Q. Li, D. Zhong, X. Peng. Wind Power Device Faults and Lightning Strikes Analysis in Hainan Oriental Wind Farm. *Wind Power.* 2010; 2010(3): 22-27.

[3] Lightning Protection of Wind Turbine Blades, CIGRE technical brochure 578, 2014.

[4] T. Shindo, M. Miki, A. Asakawa. Lightning Protection of Wind Turbine against Winter Lightning in Japan. International Conference on Lightning Protection. 2012; Vienna.

[5] IEC 61400-24, Wind turbines -Part 24: Lightning protection, 2010.

[6] Shigeru Yokoyama. Lightning protection of wind turbine blades. *Electric Power Systems Research*. 2013; 94(2013): 3-9.

[7] Amr M. Adb-Elhady, Nehmdoh A. Sabiha, Mohamed A. Izzularab. Experimental evaluation of air -termination systems for wind turbine blades. *Electric Power Systems Research*. 2014; 107 (2014): 133–143.

[8] M. Becerra, M. Longa, W. Schulzb. On the estimation of the lightning incidence to offshore wind farms. *Electric Power Research. 2018;* 157(2018): 211-226.

[9] F. Rachidi. A review of current issues in lightning protection of new generation wind-turbine blades. *IEEE Transactions on Industrial Electronics.* 2008; 55(6): 2489-2496.

[10] B. Markovski, L. Grcev, V. Arnautovski-Toseva. Transient Characteristics of Wind Turbine Grounding. International Conference on Lightning Protection. 2012; Vienna.

[11] T. Kawabata, Y. Naito, S. Yanagawa. A Development of a Measurement System Using a Rogowski Coil to Observe Sprit Lightning Current Flows Inside and Outside a Wind Turbine Generator System. International Conference on Lightning Protection. 2012; Vienna.

[12] S. Sekioka, H. Otoguro, T. Funabashi. A study on Overvoltages in Wind Tower due to Direct Lightning Stroke. International Conference on Lightning Protection. 2012; Vienna.

[13] A. C. Garolera. Lightning protection of flap system for wind turbine blades. *Ph.D. thesis.* Denmark; 2014.

[14] S. Yokoyama, Y. Yasuda, M. Minowa, S. Sekioka. Clarification of the mechanism of wind turbine blade damage taking lightning characteristics into consideration and relevant research project. International Conference on Lightning Protection. 2012; Vienna.

[15] Y. Yasuda, S. Yokoyama, M. Idenno. Verification of lightning damage classification to wind turbine blades. International Conference on Lightning Protection. 2012; Vienna.

[16] N. J. Vasa, T. Naka, S. Yokoyama. Experimental study on lightning attachment manner considering various types of lightning protection measures on wind turbine blades. International Conference on Lightning Protection. 2006; Kanazawa.

[17] A. Muto, J. Suzuki, T. Ueda. Performance comparison of wind turbine blade receptor for lightning protection. International Conference on Lightning Protection. 2010; Cagliari.

[18] A. C. Garolera, J. Holboell, S. F. Madsen. Lightning attachment to wind turbine surfaces affected by internal blade conditions. International Conference on Lightning Protection. 2012; Vienna.

[19] B. M. Radicevi , M. S. Savic, S. F. Madsen, I. Badea. Impact of wind turbine blade rotation on the lightning strike incidence -A theoretical and experimental study using a reduced-size model. *Energy.* 2012; 45(1): 644-654.

[20] A. S. Ayub, W. H. Siew, S. J. MacGregor. External lightning protection system for wind turbine blades – preliminary aerodynamic results. International Conference on Lightning Protection. 2010; Cagliari.

[21] M. Minowa, K. Ito, S. I. Sumi. A study of lightning protection for wind turbine blade by using creeping discharge characteristics. International Conference on Lightning Protection. 2012; Vienna.

[22] K. Inoue, Y. Korematsu, N. Nakamura. Study on damage-mechanism of wind turbine blades by lightning strike. International Conference on Lightning Protection. 2006; Kanazawa.

[23] Y. Goda, S. Tanaka, T. Ohtaka. Arc tests of wind turbine blades simulating high energy lightning strikes. International Conference on Lightning Protection. 2008; Uppsala.

[24] T. Ogasawara, Y. Hirano, A. Yoshimura. Coupled thermal–electrical analysis for carbon fiber/epoxy composites exposed to simulated lightning current. *Composites: Part A: Applied Science and Manufacturing*. 2010; 41(8): 973-981.

[25] P. Feraboli, M. Miller. Damage resistance and tolerance of carbon/epoxy composite coupons subjected to simulated lightning strike. *Composites: Part A: Applied Science and Manufacturing*. 2009; 40(6): 954–967.

[26] Y. F. Liao, S. R. Wang, Z. Y. Luo, H. Tan, C. J. Yu, J. S. Zhou , K. F. Cen. Research on cellulose rapid pyrolysis. *Journal of Zhejiang University (Engineering Science).* 2003; 37(5): 582-587.

TABLE I

INITIAL BREAKDOWN VOLTAGE UNDER DIFFERENT EXPERIMENTAL CASES (NEGTIVE VOLTAGE, UNIT IN kV)

Upper electrode position	1	2	3	4	5	6
A	260	280	260	240	240	220
B	240	260	240	220	260	240
C	220	240	220	180	240	220

TABLE II

INITIAL BREAKDOWN VOLTAGE UNDER DIFFERENT EXPERIMENTAL CASES (POSITIVE VOLTAGE, UNIT IN kV)

Upper electrode position	1	2	3	4	5	6
A	260	260	240	220	240	200
B	240	240	220	220	240	220
C	240	220	200	180	200	180

TABLE III

TOLERANCE RATIO OF THE SANDWICHED MATERIALS (%)

Samples	PVC sandwich	PET sandwich	Balsa wood sandwich
199.5J	98.3	98.3	99.4
1795.5J	0	0	84.3
3192J	0	0	34.5

TABLE IV

TOLERANCE RATIO OF THE COMBINED STRUCTURE (%)

Samples	PVC combination	PET combination	Balsa wood combination
199.5J	97.5	98.75	99.6
1795.5J	92.5	95	99
3192J	0	25	76

TABLE V

CHARACTERISTIC PARAMETERS OF THE CORE MATERIALS

Materials	PVC	PET	balsa wood
Porosity(%)	95	93	94
Thermal conductivity(W/ $m^{-1}k^{-1}$)	0.14	0.15	0.16
Glass transition temperature(K)	355	340	543
Density(g/cm^3)	1.38	1.38	1.5
Water moisture(%)	1.2	1.64	5.4

a) materials carbonization b) blade cracking

Fig. 1. Blade damage resulting from lightning strikes.

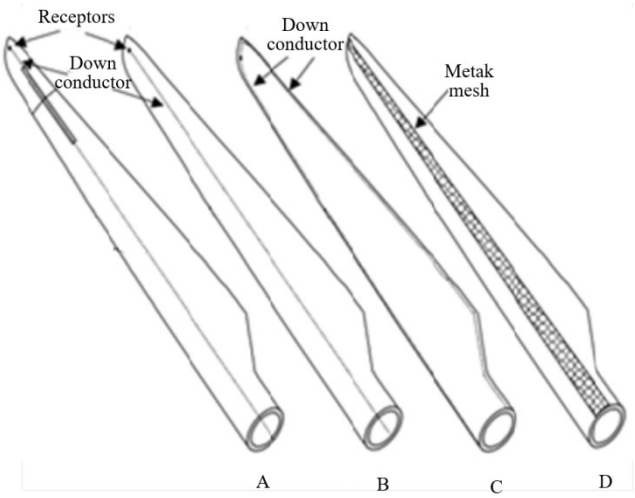

Fig. 2. Schematic diagrams showing different designs of lightning protection for wind turbine blade.

a) Real blade

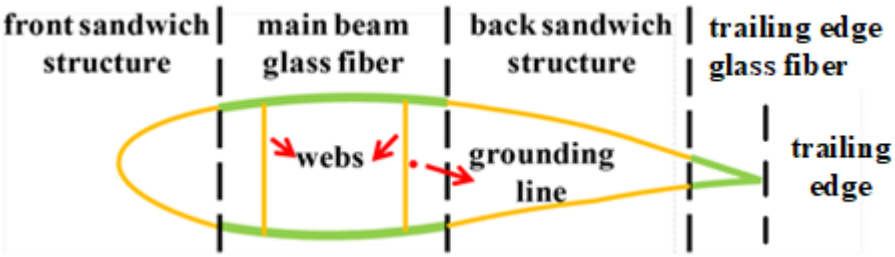

b) Cross-sectional view of the blade

Fig. 3. The structure and constituting components of a typical wind turbine blade.

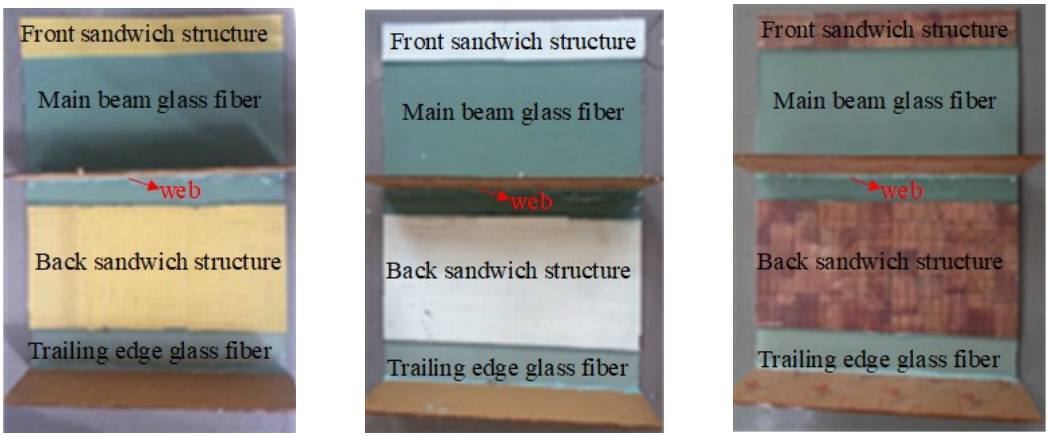

a)Sample A b) Sample B c) Sample C

Fig. 4. Structure of the model blades used in tests. a) Blade with PVC, b) blade with PET, c) blade with balsa wood

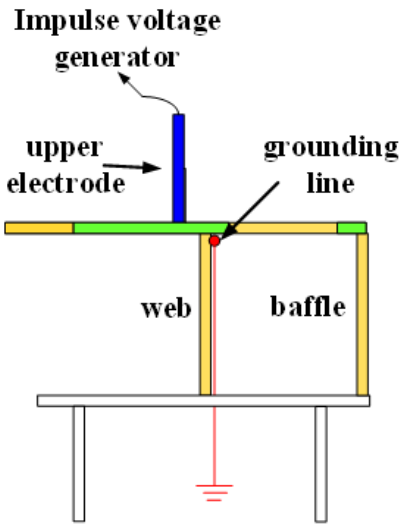

Fig. 5 Impulse Experiment setup.

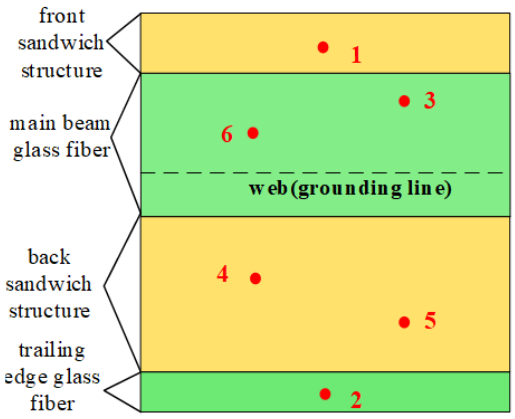

Fig. 6. The Upper electrode position (red points 1-6, sample A as an example)

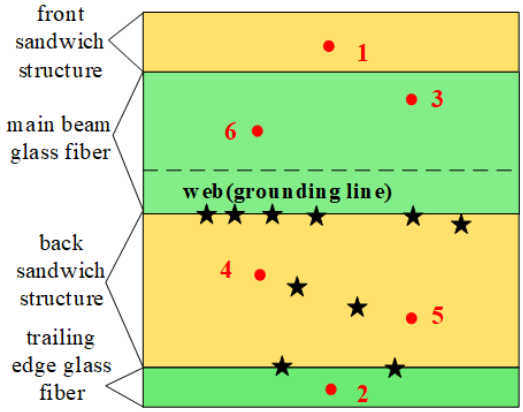

a) sample A

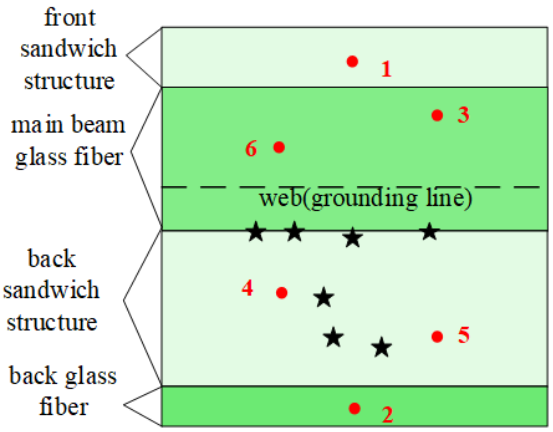

b) sample B

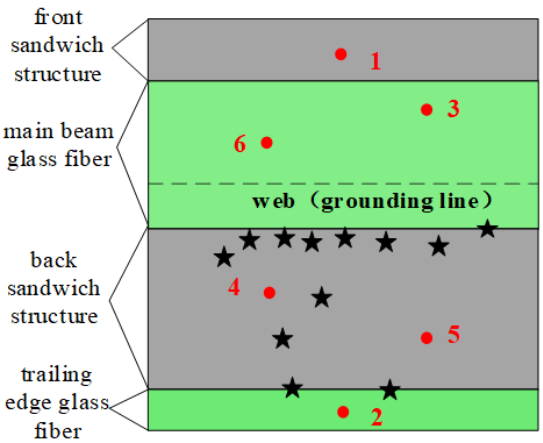

c) sample C

Fig. 7. Breakdown point distribution under negative voltage for different electrode positions (black stars)

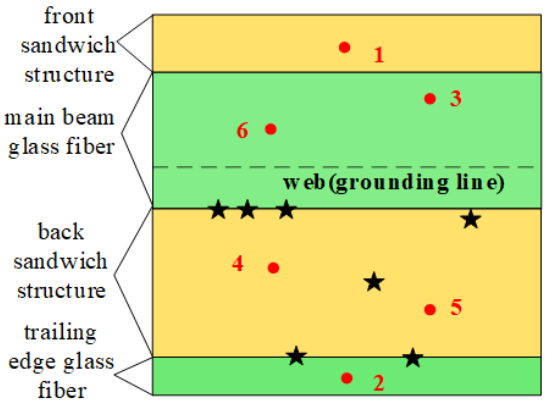

a) Sample A

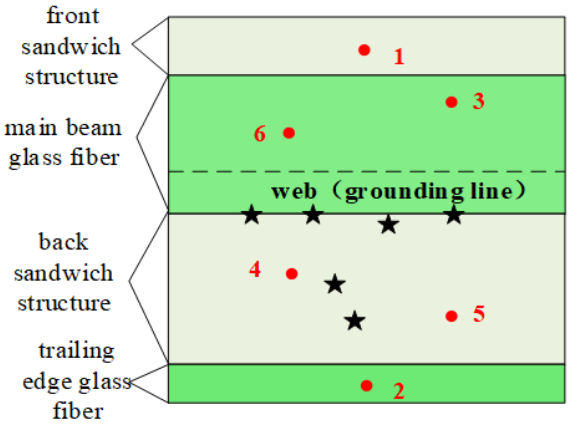

b) Sample B

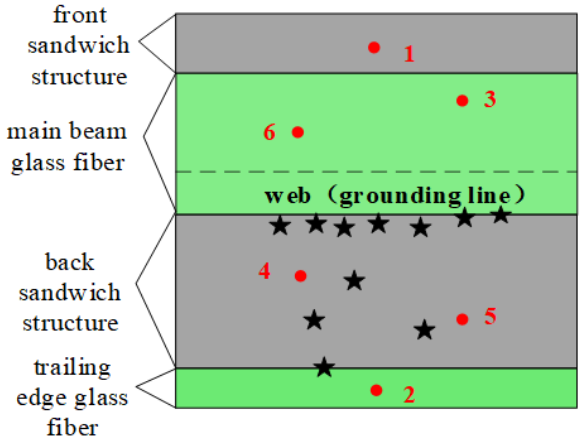

c) Sample C

Fig. 8. Breakdown point distribution under positive voltage for different electrode positions (black stars).

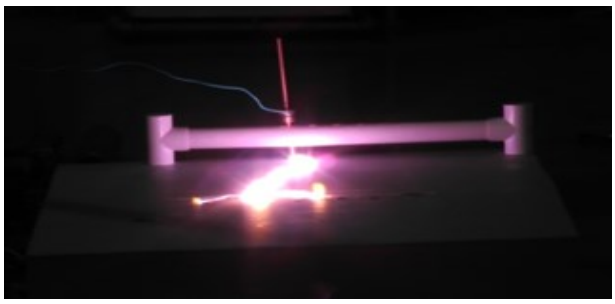

a) Position 1(440kV, negative voltage,)

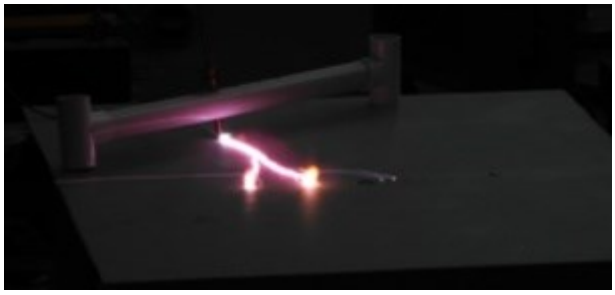

b) Position 3 (350kV, negative voltage)

Fig. 9. Multiple arc paths of Sample C with balsa wood

a) PVC sandwich

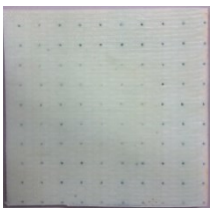

b) PET sandwich

c) Balsa wood sandwich

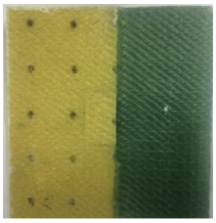

d) PVC combination

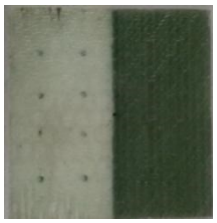

e) PET combination

f) Balsa wood combination

Fig. 10. Different test samples prepared for lightning discharge study.

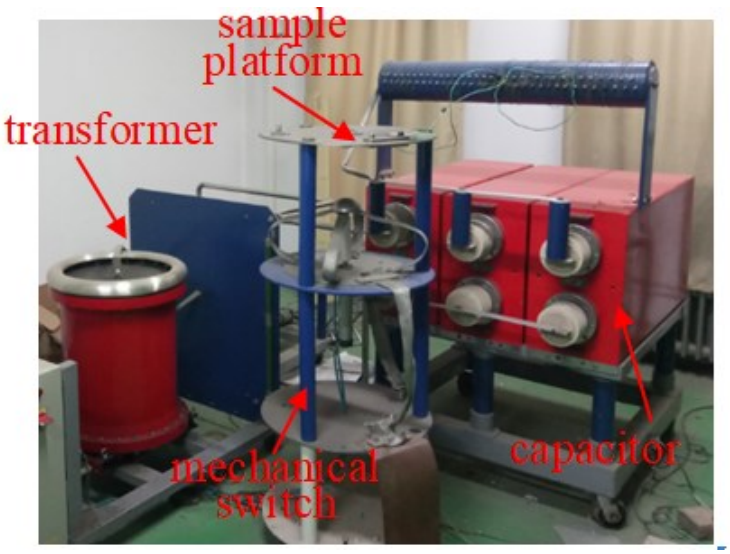

Fig. 11. Experimental setup for impulse current arc discharge.

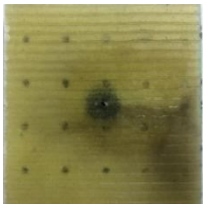

a) PVC 199.5J

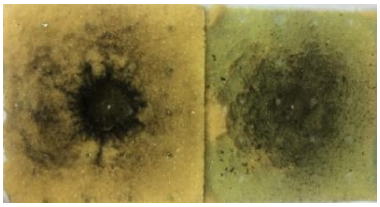

b) PVC 1795.5J

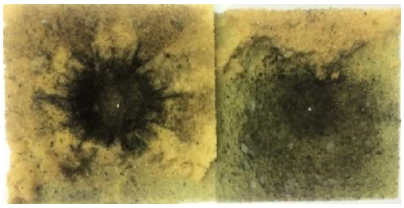

c) PVC 3192J

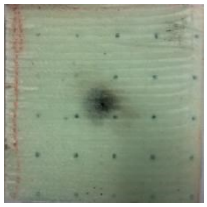

d) PET 199.5J

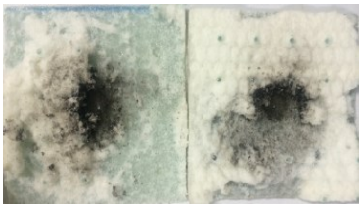

e) PET 1795.5J

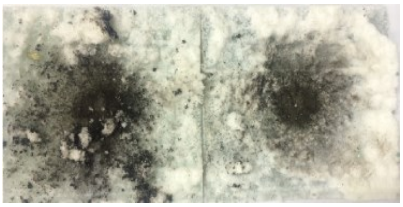

f) PET 3192J

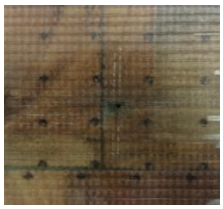

g) Balsa wood 199.5J

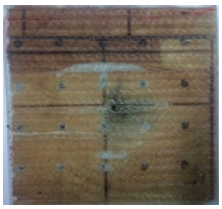

h) Balsa wood 1795.5J

i) balsa wood 3192J

Fig. 12. Damage morphology of different sandwich structure

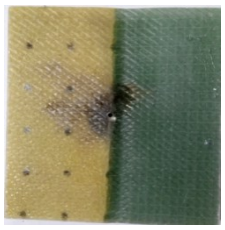

a) PVC combination 199.5J

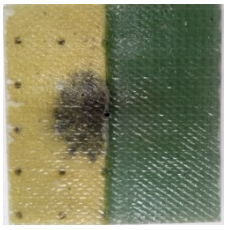

b) PVC combination 1795.5J

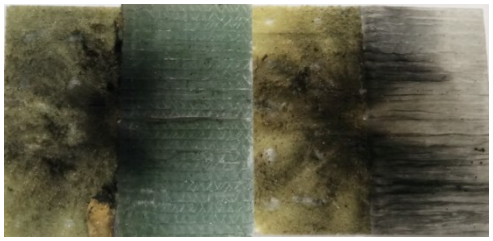

c) PVC combination 3192J (complete layering)

Fig. 13. Damage morphology of the PVC combination

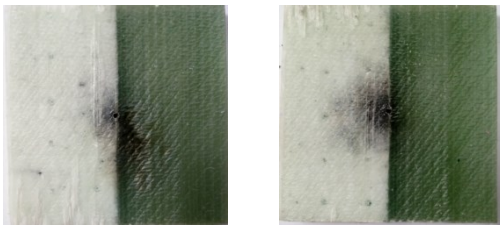

a) PET combination 199.5J b) PET combination 1795.5J

c) PET combination 3192J and cross section

Fig. 14. Damage morphology of the PET combination (hybrid type).

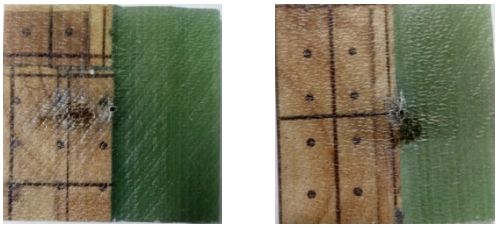

a) Balsa wood combination 199.5J b) Balsa wood combination 1795.5J

c) Balsa wood combination 3192J and the cross section

Fig. 15. Damage morphology of the balsa wood combination

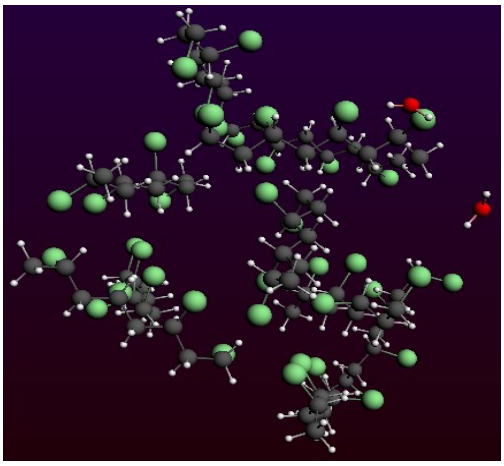

a) PVC

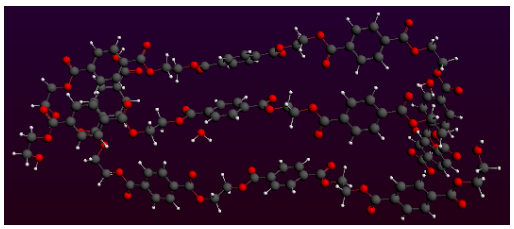

b) PET

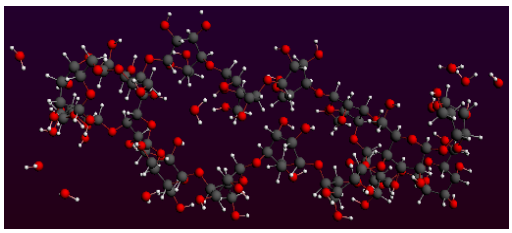

c) Balsa wood

Fig. 16. Molecular models of the three core materials

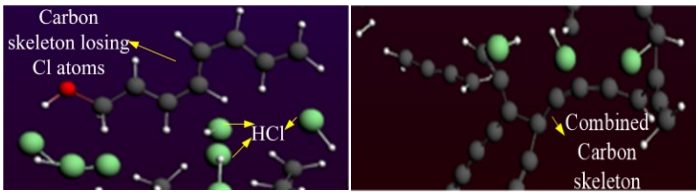

a) PVC 498K b) PVC 2989K

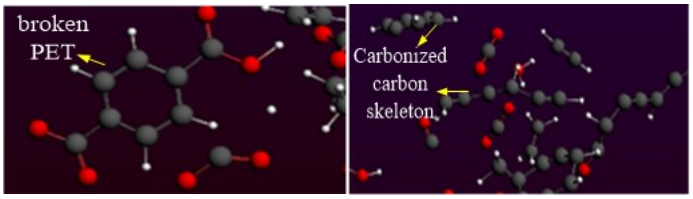

b) PET 498K d) PET 2989K

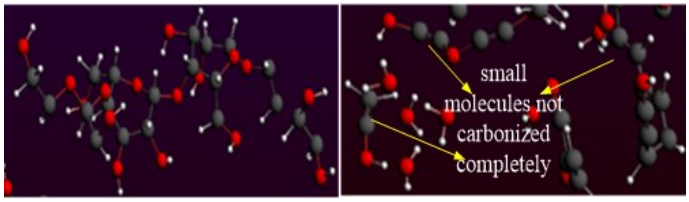

e) Balsa wood 498K f) Balsa wood 2989K

Fig. 17. RMD simulation results of the materials' pyrolysis process

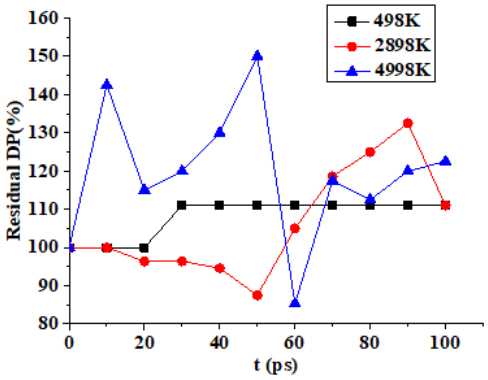

a) PVC

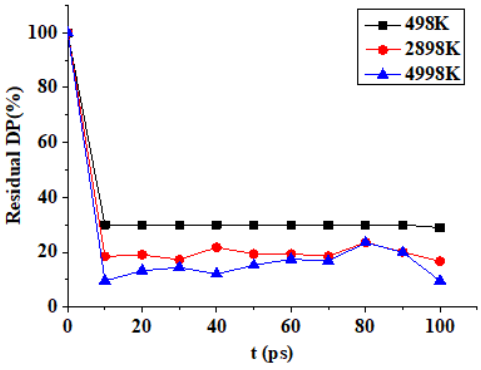

b) PET

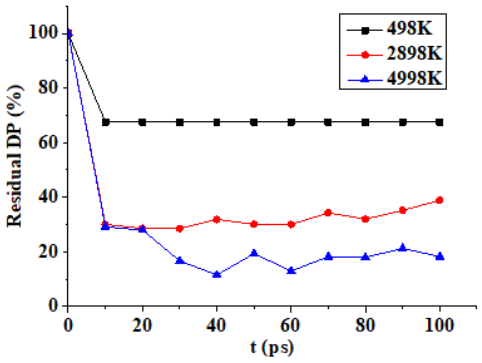

c) Balsa wood

Fig. 18. Residual DP of the large polymer molecules

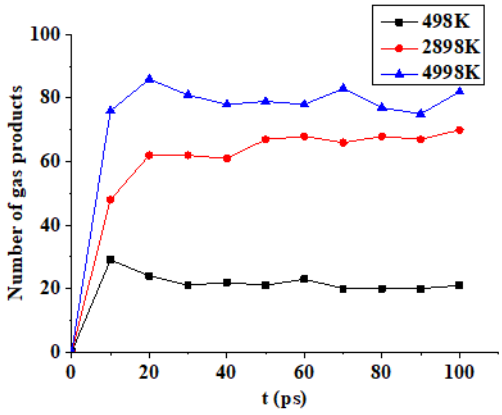

a) PVC

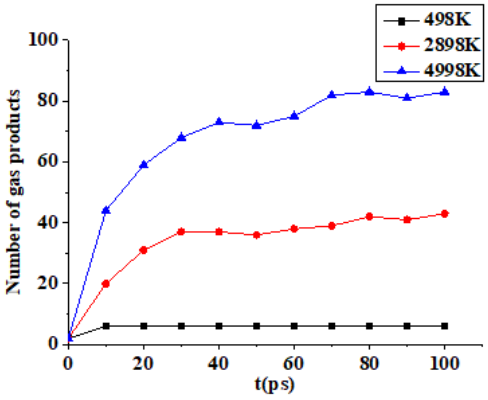

b) PET

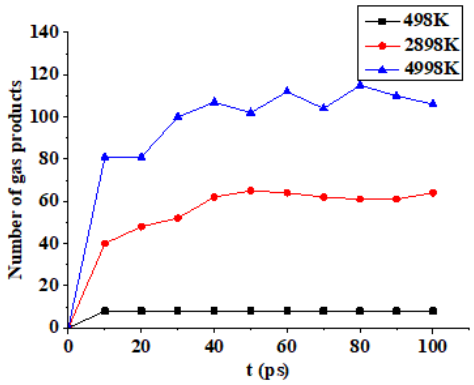

c) Balsa wood

Fig. 19. Number of gas products predicted by molecular simulation.